Effect of Sterol Regulatory Element Binding Protein-1a on the Mitochondrial Protein Pattern in Human Liver Cells Detected by 2D-DIGE

Stefan Lehr,[‡] Jorg Kotzka,[‡] Haluk Avci,[‡] Birgit Knebel,[‡] Stefan Muller,[§] Franz G. Hanisch,[§] Sylvia Jacob,[‡] Claudia Haak,[‡] Fransiscus Susanto,[‡] and Dirk Muller-Wieland*[,‡]

Institute for Clinical Biochemistry and Pathobiochemistry, German Diabetes Center, Heinrich-Heine-University Düsseldorf, and Leibniz Center for Diabetes Research, Düsseldorf, Germany, and Center for Molecular Medicine, University of Cologne, Cologne, Germany

Received September 21, 2004; Revised Manuscript Received January 26, 2005

ABSTRACT: Sterol regulatory element binding protein-1a (SREBP-1a) is a transcription factor that is a major player in lipid metabolism and insulin action. We have generated human liver cells (HepG2) overexpressing active SREBP-1a constitutively called SREBP-1a (+). These cells show massive intracellular lipid accumulation. To elucidate the effect of SREBP-1a on lipid metabolism at the level of the cellular protein network, we have analyzed the protein pattern of mitochondria using the novel technique two-dimensional difference gel electrophoresis (2D-DIGE). Mitochondria were enriched by subcellular fractionation using differential and isopyknic centrifugation. Proteins of isolated organelles were labeled with Cy dyes and separated on 2D gels. These gels revealed more than 100 protein spots, which were significantly different in their abundance between wild-type and SREBP-1a (+) cells. MALDI mass spectrometry showed that 68% of identified proteins belong to mitochondria. In SREBP-1a (+) cells, several enzymes involved in lipid metabolism were significantly altered, suggesting that cellular lipid metabolism is triggered by accumulation of fatty acids rather than by its degradation. To test the possible functional relevance of this finding, intracellular fatty acid (FA) patterns were analyzed by gas chromatography. The results showed a significant increase in total fatty acid content with a shift in composition to long-chain unsaturated FAs. Therefore, the detected protein differences might be an explanation for the observed intracellular lipid accumulation and might link SREBP-1a to features like steatosis hepatis.

Sterol regulatory element binding proteins (SREBPs) are a family of basic helix−loop−helix transcription factors that are embedded as precursor proteins in the endoplasmic reticulum and nuclear envelope. To date, three SREBP isoforms have been detected: SREBP-1a, SREBP-1c (shorter splicing variant of SREBP-1a), and SREBP-2 (*1*−*5*). Activation of SREBPs initiated by cellular cholesterol depletion is mediated by sequential cleavage (*6*). As a result, the amino-terminal domain of the protein translocates into the nucleus and initiates, activated by phosphorylation (*7*−*10*), transcription of a wide range of target genes, e.g., genes involved in cholesterol biosynthesis (HMG-CoA synthase, HMG-CoA reductase, and farnesyldiphosphate synthase), lipid catabolism (LDL receptor and lipoprotein lipase), fatty acid synthesis (acetyl-CoA carboxylase, fatty acid synthase, stearoyl-CoA desaturase 1, and gylcerol-3-phosphats acyltransferase), intracellular transport (caveolin-1 and caveolin-2), and signal transduction (leptin) (*11*). In function, SREBP-2 seems to be the major regulator of cholesterol homeostasis, whereas SREBP-1c regulates predominantly de novo synthesis of fatty acids. In contrast, SREBP-1a seems to influence both lipogenic and cholesterogenic enzymes (*12*).

For lipid metabolism, the mitochondrial compartment represents a central organelle within the cell. According to this, we investigated the effect of SREBP-1a on the mitochondrial subprotein pattern. Therefore, protein pattern analyses by two-dimensional gel electrophoresis and mass spectrometry provide a powerful tool for elucidating changes at the level of protein expression (*13*, *14*). In this study, we processed mitochondrial protein samples obtained from wild-type and HepG2 cells stably overexpressing the constitutively active N-terminal domain of SREBP-1a on two-dimensional gels utilizing the two-dimensional difference gel electrophoresis (2D-DIGE) system (*15*). This approach allows the highest accuracy and statistical confidence in measurements of protein abundance (*16*, *17*).

EXPERIMENTAL PROCEDURES

Plasmids and Molecular Cloning. Cloning of the expression vector (pcDNA3.1/HisA, Invitrogen) containing the N-terminal domain of human SREBP-1a (amino acids 1−460, SREBP-1a-NT) was described previously (*8*). To construct pcDNA3/HA-SREBP-1a-NT, a hemagglutinin (HA) tag was added to the 5′-end of the SREBP-1a-NT construct (pcDNA3.1/HisA-SREBP-1a-NT) after linearization with

* To whom correspondence should be addressed: Institute of Clinical Biochemistry and Pathobiochemistry, German Diabetes Center, Auf'm Hennekamp 65, 40225 Düsseldorf, Germany. Telephone: 49-211-3382-240. Fax: 49-211-3382-430. E-mail: mueller-wieland@ddfi.uni-duesseldorf.de.

[‡] Heinrich-Heine-University Düsseldorf and Leibniz Center for Diabetes Research.

[§] University of Cologne.

10.1021/bi0479656 CCC: $30.25
Published on Web 03/08/2005

BamHI by PCR after deletion of the His tag and the first codon of SREBP-1a using the following primers: sense primer (underlined bases represent the DNA sequence of the HA peptide and bold underlined bases the DNA sequence of SREBP-1a), 5′-GGATCCATGTACCCATACGACGTCCCAGACTACGCT**GACGAGCCACCCTTC**-3′; and antisense primer (vector sequence of pcDNA3.1/HisA, nucleotides 919−896), 5′-GGTAAGCTTAAGTTTAAACGCTAG-3′. After amplification, the PCR mixture was digested with DpnI followed by religation. The sequence of the construct was confirmed by using a model 3100 DNA sequencer (Applied Biosystems Inc.).

Cell Culture and Stable Transfection of HepG2 Cells. Human hepatoma cells (HepG2) were maintained in culture medium [RPMI 1640 medium (Sigma-Aldrich) supplemented with 10% (v/v) fetal calf serum (FCS) (GibcoBRL) and antibiotics (GibcoBRL)]. To establish HepG2 cells stably expressing SREBP-1a-NT, cells were transfected with pcDNA3/HA-SREBP-1a-NT; these cells will be named SREBP-1a (+) cells. For control, HepG2 cells were transfected with the pcDNA3 expression vector, named HepG2-pcDNA3. Before transfection, cells were released by trypsinization, washed with 1× PBS, and resuspended in Opti-MEM (GibcoBRL) supplemented with 10% (v/v) FCS. Subsequently, the cell suspension (5×10^6 cells) was mixed with pcDNA3/HA-SREBP-1a-NT (2.5 μg), transferred to an electroporation cuvette (inter electrode distance of 0.4 cm, Bio-Rad), and pulsed for 18 ms in a GenePulser II (Bio-Rad). Before the cells were seeded on six-well plates (Greiner bio-one), the cell suspension was diluted with culture medium. Two days after transfection, cells were selected by growth in culture medium containing 800 μg/mL G418 (Sigma-Aldrich). After 20 days, individual G418-resistant colonies of HepG2-pcDNA3 and SREBP-1a (+) cells were selected and expanded in culture medium containing 500 μg/mL G418.

Laser Scanning Microscopy. HepG2-pcDNA3 and SREBP-1a (+) cells were seeded onto glass coverslips and maintained for 3 days in culture medium (RPMI 1640 with 10% FCS). When cells reached the desired confluence, the medium was removed from the dish and the prewarmed culture medium containing the cell permeable mitotracker red CMxRos (Molecular Probes) was added at a concentration of 250 nM. After staining had been carried out for 45 min at 37 °C, cells were washed with culture medium. Subsequently, cells were fixed in culture medium containing 4% (w/v) formaldehyde (from paraformaldehyde) for 15 min at 37 °C. Following two washes in 1× Mg-PBS, cells were permeabilized in Hepes−Triton permeabilization buffer [20 mM Hepes, 300 mM sucrose, 50 mM NaCl, 3 mM $MgCl_2$, and 0.5% (v/v) Triton X-100 (pH 7.4)] for 10 min at −20 °C. The permeabilization buffer was removed, and 2 mL of 1× Mg-PBS containing 1% fatty acid-free BSA [Mg-PBS/BSA (w/v)] was added. After incubation for 30 min at room temperature, the Mg-PBS/BSA solution was replaced with a buffer containing 2 μg/mL anti HA-fluorescein (HA-FITC) rat monoclonal antibody (clone 3F10, Roche). After incubation for 1 h at room temperature, the coverslips were washed twice with 2 mL of a Mg-PBS/BSA solution for 15 min each and mounted on microscope slides with 90% (v/v) glycerol, 50 mM Tris-HCl (pH 9.0), and 2.5% (w/v) 1.4-diazadicyclo-[2.2.2]octane. Fluorescence microscopy was performed with a 63× planapochromat oil immersion objective and a standard FITC filter set (BP, 505−530 nm; LP, 560 nm). The cells were visualized using an Axiovert 200M microscope (Zeiss AG) equipped with an LSM 5 Pascal laser scanning confocal microscope using a gas argon/HeNe laser. Images of red−green doubly labeled cells were acquired in a multitrack configuration; i.e., the wavelengths are scanned sequentially, switching between wavelengths.

Histomorphology. For imaging cellular morphology, HepG2-pcDNA3 and SREBP-1a (+) cells were seeded into 3 cm dishes (1×10^6 cells/dish) and grown as a monolayer in culture medium [RPMI 1640 medium (Sigma-Aldrich) supplemented with 20% (v/v) fetal calf serum (FCS) (GibcoBRL), antibiotics (GibcoBRL), and 10 mM glucose] for 9 days [37 °C, 5% CO_2 (v/v)]. For characterization of histomorphology, fixed slides were stained in Mayer's hemalaun solution (Merck) according to the manufacturer's instructions. Stained slides were embedded in glycerol-gelatine and mounted with glass slips.

Relative Quantification of Lipogenic Genes by Real-Time PCR. Total RNA of HepG2-pcDNA3 and SREBP-1a (+) cells was extracted with the RNA Mini Spin Kit (Qiagen). The RNA integrity and amount were evaluated by using the RNA Nano Chip according to manufacturer's instructions (Agilent). For reverse transcription, 1 μg of total RNA was used (MMVRT, Promega). Real-time PCR was performed in triplicate with the cDNA equivalent of 20 ng of reverse-transcribed RNA per reaction. For detection of SREBP-1 and SREBP-2, specific primers and FAM-labeled specific hybridization probes were used (Assay on Demand, Applied Biosystems). For detection of the stably expressed SREBP-1a, a HA-Tag specific hybridization probe was used with a 5′-primer located on the vector backbone (T7 sequencing primer) and a 3′-primer in SREBP-1a. Primer and probes for all other transcripts investigated were purchased as prepared assays (Assay on Demand, Applied Biosystems). RT-PCR was performed under standardized conditions (2× Universal PCR Mastermix, Applied Biosystems) with the ABI Prism 7000 Sequence Detection System. Data were normalized to 18S content and further analyzed according to the $\Delta\Delta C_t$ method.

Subcellular Fractionation. For the preparation of mitochondria, HepG2-pcDNA3 and SREBP-1a (+) cells were seeded into 14.5 cm dishes (1×10^7 cells/dish) and grown as a monolayer in culture medium under standardized conditions [RPMI 1640 medium (Sigma-Aldrich) supplemented with 10% (v/v) fetal calf serum (FCS) (GibcoBRL) and antibiotics] for 4 days [37 °C, 5% CO_2 (v/v)]. Thereafter, cells were washed twice in a NaCl solution [0.9% (w/v), pH 7.5] and harvested by being scraped off in a NaCl solution. After centrifugation (800*g* for 5 min at 4 °C), the pelleted cells were resuspended in 10 volumes of homogenization buffer [10 mM Tris-HCl (pH 7.4), 225 mM mannitol, 75 mM sucrose, 0.5 mM EGTA, and 0.5 mM DTT] and homogenized with a Dounce homogenizer on ice (10 strokes). Cell debris was removed by centrifugation (666*g* for 20 min at 4 °C), and subsequently, mitochondria were sedimented from the supernatant (11000*g* for 20 min at 4 °C). This raw mitochondria fraction was washed two times in 1 mL of homogenization buffer and re-isolated by another centrifugation (11000*g* for 20 min at 4 °C). The resulting pellet was resolved in 2 mL of resuspension buffer

[10 mM Tris-HCl (pH 7.4), 250 mM sucrose, 0.5 mM EGTA, and 0.5 mM DTT] and applied onto a linear sucrose gradient [30 mL, from 0.7 to 1.5 M, 10 mM Tris-HCl (pH 7.4)] centrifuged in a swing-out bucket (SW 28 Beckman Coulter, 80000*g* for 60 min at 4 °C). After that, the sucrose gradient was pressed out in 2 mL fractions, using a saturated sucrose solution. Fractions representing the largest amount of mitochondria were diluted with 5 volumes of resuspension buffer, pooled, and sedimented (14000*g* for 10 min at 4 °C). Prepared mitochondria were consecutively washed [0.9% (w/v) NaCl solution (pH 7.5)] and subjected to 2D-DIGE analysis. All preparation steps were monitored by marker enzyme activity, JC-1 dye uptake, and electron microscopy. Protein concentrations generally were measured using the Bio-Rad DC protein assay.

Marker Enzyme Assays. The mitochondria quality of all preparation steps was monitored by assessing organelle specific marker enzymes according to the specified citations as follows: succinate dehydrogenase, mitochondria (*18*); alkaline phosphatase, plasma membrane; glucose-6-phosphatase, endoplasmic reticulum; acidic phosphatase, lysosomes (*19*); and catalase, peroxisomes (*20*).

Mitochondria Vitality Assay. The vitality of mitochondria was assessed by the uptake of JC-1 (5,5′,6,6′-tetrachloro-1,1′,3,3′-tetraethylbenzimidazolcarbocyanine iodide) into mitochondria using the MitoIso1-Kit (Sigma-Aldrich) according to the manufacturer's recommendations.

Electron Microscopy. Samples (approximately 5 mg) were fixed in 3% (v/v) glutaraldehyde overnight and washed with cacodylate buffer [290 mM sodium cacodylate (pH 7.4)]. Samples were consecutively contrasted with osmium tetroxide [2% (w/v) in cacodylate buffer] and uranyl acetate [2% (w/v)]. To gain an impression of the quality of organelle preparation, samples were precipitated in the presence of BSA [5% (w/v)] and overlaid with one droplet of glutaraldehyde [25% (v/v)]. The gelatinized sample was dissected with a scalpel and dehydrated with series of increased concentrations of alcohol. After being embedded in 2,5-dioxotetrahydrofuran, the preparations were cut into 60 nm slices with an ultramicrotome (UMU III) and then analyzed on a Zeiss TEM 910 electron microscope.

Two-Dimensional Difference Gel Electrophoresis (2D-DIGE). The organelle pellet was solubilized in lysis buffer [25 mM Tris, 4% CHAPS (w/v), 8 M urea, and 2 M thiourea] and set to a final protein concentration of 2 mg/mL. After brief sonication, insoluble material was removed by centrifugation at 40000*g* (40 min at 4 °C). The protein labeling with cyanine dyes was performed according to the manufacturer's (Amersham biosciences) instructions. Briefly, 50 μg (25 μL) of proteins per gel of either sample, which should be compared, was labeled with 400 pmol of dye (Cy3 or Cy5). A pool of the two samples (25 μg each per gel) was labeled with 400 pmol of Cy2 to function as internal standard on each gel. To eliminate dye specific differences, each sample was labeled cross-wise with Cy3 and Cy5. Prior to isoelectric focusing (IEF), the labeled samples were filled with an equal volume (25 μL each per gel approach) of lysis buffer containing 2% (w/v) DTT and 2% (v/v) IPG buffer (Amersham Biosciences).

Labeled samples were combined (50 μg each labeled with Cy3, Cy5, and Cy2 per gel) and subjected to IEF on a MultiPhor II electrophoresis unit (Amersham Biosciences) using IPG strips (24 cm, pH 4−7 linear) according to the manufacturer's recommendations. In detail, IPG strips were rehydrated overnight in 2% CHAPS (w/v), 0.4% DTT (w/v), 8 M urea, 2 M thiourea, and 0.5% corresponding IPG buffer (v/v). Samples were applied adjacent to the acidic end of the IPG strips by cup loading. IEF conditions were as follows: 3 h at 300 V, followed by a gradient of 10 V/min up to 3500 V, and then 21 h at 3500 V (20 °C).

Prior to second-dimension separation, IPG strips were equilibrated for 15 min in 50 mM Tris-HCl (pH 8.8), 6 M urea, 30% (v/v) glycerol, and 2% (w/v) SDS containing 0.5% (w/v) DTT. Strips were then re-equilibrated for 15 min in the same buffer containing 4.5% (w/v) iodoacetamide instead of DTT.

For protein separation by size in the second dimension, 1.0 mm thick linear 12.5% polyacrylamide gels (24 cm × 18 cm) combined with a Tris (0.1 M)/Tricine (0.1 M) buffer system were used. Electrophoresis of 12 large format gels was conducted simultaneously at 2 W/gel and 25 °C on an EttanDalt 12 system (Amersham Biosciences).

Immediately, gels were scanned directly between the glass plates using a Typhoon 9400 (Amersham Biosciences) laser scanner according to the manufacturer's recommendations (resolution of 100 μm, photomultiplier tube of 550 V). For spot picking, gels were subsequently stained with colloidal coomassie.

Image Analysis. Determination of protein spot abundance and statistics was carried out automatically using DeCyder version 5.0 (Amersham Biosciences). For DeCyder, analysis gels (four replicates, two labeled with Cy3 and two with Cy5) containing the identical sample were grouped for comparison. Selection criteria for detection of significant changed protein spots were as follows. First, protein spots have to present in all analyzed gels; second, the standardized average spot volume ratios exceeded 1.5 (*t* test value of $<10^{-3}$ in four parallel gels).

Protein Identification. Protein spots of interest were excised from colloidal coomassie restained gels using a skin biopsy punch (∅ = 1 mm). Gel pieces were washed in digestion buffer (10 mM ammonium bicarbonate) and digestion buffer and acetonitrile (1:1, v/v) for 10 min three times each. After being dried with acetonitrile, gel pieces were reswollen with 5 μL of 10 mM ammonium bicarbonate containing 10 ng/μL trypsin (Invitrogen) and incubated for 30 min at 4 °C. Then protein digestion was performed overnight at 37 °C. The resulting peptides were eluted with 10 μL of 0.1% TFA in an ice/water mixture by sonicating for 5 min; 0.4 μL of extracted peptides was directly applied on a MALDI AnchorChip target (600 μm, Bruker) and mixed with a dihydroxybenzoic acid solution [2,5-dihydroxybenzoic acid (5 mg/L) in acetonitrile and 0.1% (w/v) TFA (1:2, v/v)]. Samples were analyzed in a time-of-flight Reflex IV mass spectrometer (Bruker) equipped with a reflector and delayed extraction. Calibrated and annotated spectra were subjected to a Protein Data Bank search (Mascot search engine). Criteria for protein identification were as follows: Mascot score higher than 80, mass tolerance of 150 ppm. Calculated pI and molecular mass data were obtained by Mascot.

Determination of the Cellular Fatty Acid Composition by Gas Chromatography (GC). For determination of the lipid composition, HepG2-pcDNA3 and SREBP-1a (+) cells were seeded into 14.5 cm dishes (1×10^7 cells/dish) and grown

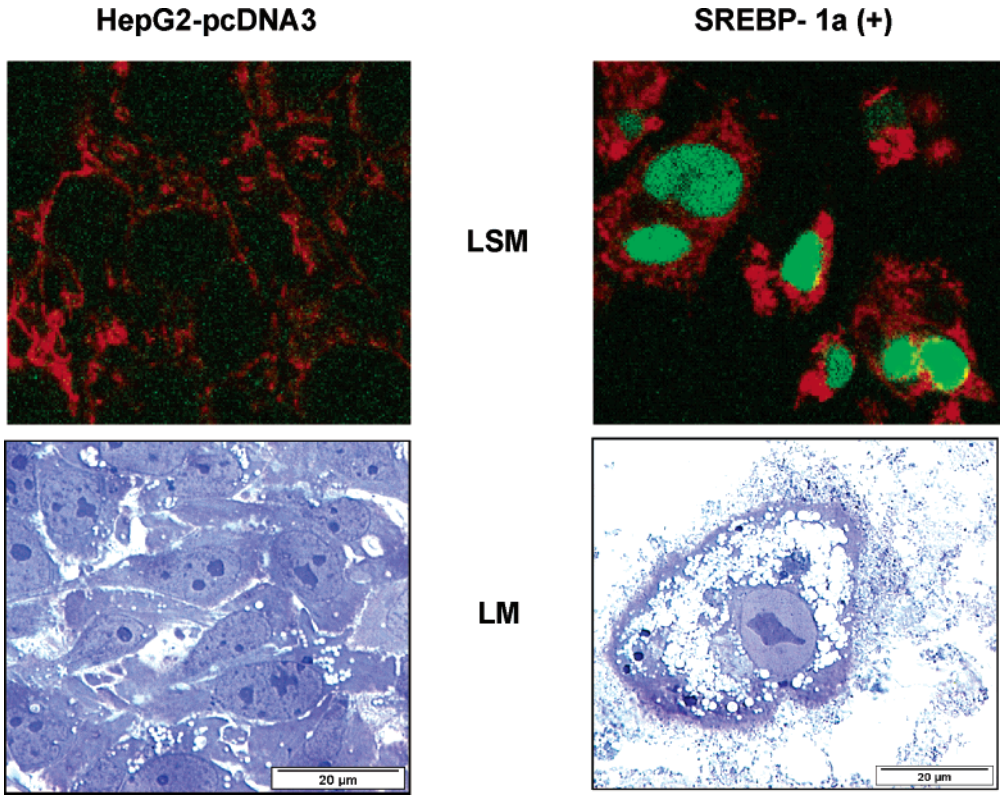

FIGURE 1: Histomorphology of SREBP-1a (+) cells. (LSM) Typical laser scanning micrograph of HepG2-pcDNA3 and SREBP-1a (+) cells seeded onto glass cover slips and maintained for 3 days in culture medium (RPMI 1640 supplemented with 10% FCS). Localization of overexpressed SREBP-1a and distribution of mitochondria were investigated by probing cells simultaneously with an anti-HA-fluorescein (HA-FITC) antibody (2 μg/mL) and mitotracker red CmxRos (250 nM) as described in Experimental Procedures. (LM) For imaging cellular morphology, 1×10^6 cells were seeded into a 3 cm dish and grown as a monolayer in culture medium (RPMI 1640) supplemented with 20% FCS and 10 mM glucose for 9 days. For light microscopy, cells were stained with Mayer's hemalaun (Merck) according to the manufacturer's instructions.

as monolayers in culture medium under standardized conditions [37 °C, 5% CO_2 (v/v)] for 4 days. Thereafter, cells were washed twice in a NaCl solution [0.9% (w/v), pH 7.5] and harvested by being scraped off in a NaCl solution. After centrifugation (800*g* for 5 min at 4 °C), the pellet was subjected to fatty acid quantification. For the determination of free fatty acid (FFA) content, 50 μg of margaric acid as an internal standard was added to the pellet. To denaturate proteins, 2 mL of a 2-propanol/1 M H_2SO_4 [40:1 (v/v)] mixture and 4 mL of *n*-hexane were added. The sample was vortexed (30 s) and thereafter centrifuged for 5 min at 3000*g*. Subsequently, the organic layer was completely evaporated under a steam of nitrogen. For determination of the total fatty acid (TFA) content, 50 μg of pentadecanoic acid as an internal standard was added to the pellet. For saponification of the cell lipids, 1 mL of methanolic NaOH was used. The tubes were tightly capped and were allowed to incubate for 1 h at 90 °C in a heating block. The reaction mixture was cooled to room temperature, and 5 mL of *n*-hexane was added. After the solution was shaken on a vortex mixer, the sample was centrifuged (5 min at 3000*g*) and the *n*-hexane layer was removed. The mixture was neutralized with concentrated HCl, and then 2 mL of a 2-propanol/1 M H_2SO_4 [40:1 (v/v)] mixture was added. Then, 4 mL of *n*-hexane was added. After that, the solution was vortexed for 30 s and denatured proteins were pelleted (5 min at 3000*g*). The organic layer was completely evaporated under a steam of nitrogen. The residues of TFA or FFA preparation were resolved in 100 μL of methanolic hydrogen chloride and incubated for 15 min at 60 °C for preparing methyl ester derivates of fatty acids. Again, the reaction mixture was evaporated under nitrogen to complete dryness, and the residue was reconstituted in 50 μL of *n*-hexane. For gas chromatography, a 1 μL sample was injected into the gas−liquid chromatographic system. The chromatograms were recorded on a Packard model 439 gas−liquid chromatograph equipped with a flame ionization detector and a 60 m Hewlett-Packard fused silica capillary column coated with FS-FFAB-CB-0,25. Nitrogen was used as the carrier gas at a flow rate of 4 mL/min. The injector block and detector were held at 250 °C. The column temperature was set at 100 °C for 1 min initially and then increased to 220 °C at a rate of 2 °C/min.

RESULTS

Sterol regulatory element binding protein-1a (SREBP-1a) is a transcription factor that is a major player in lipid metabolism. To dissect the role of SREBP-1a in cellular physiology and especially in the mitochondrial protein pattern, we have generated a human liver cell line stably overexpressing the mature form of SREBP-1a (amino acids 1−460).

Effect of SREBP-1a on Cellular Lipid Content. Quantitation of SREBP-1 in SREBP-1a (+) cells by real-time PCR showed a more than 2-fold increase in the level of SREBP-1 (Figure 2). To distinguish the overexpressed SREBP-1a from endogenous SREBP-1, a specific probe for the HA tag was

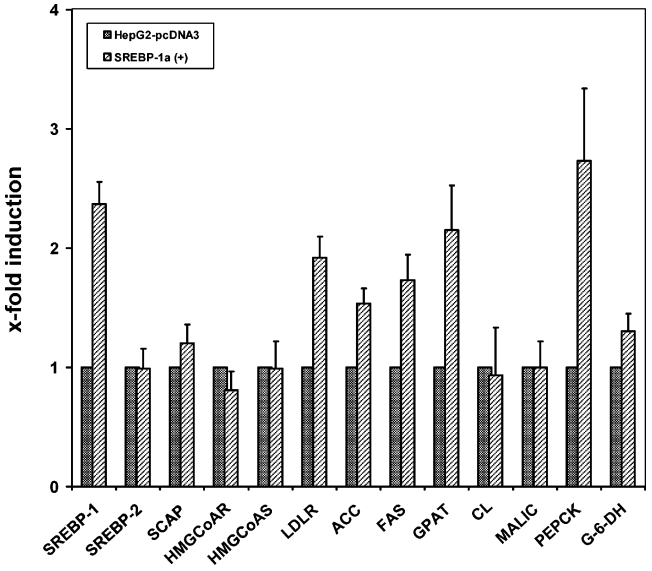

FIGURE 2: RNA expression levels of metabolic key enzymes in SREBP-1a (+) cells. For preparation of total RNA, HepG2-pcDNA3 and SREBP-1a (+) cells were maintained for 4 days in culture medium (RPMI 1640 supplemented with 10% FCS). RNA expression levels of key enzymes were determined by real-time PCR using specific probes. The following enzymes were analyzed: SREBP-1, SREBP-2, sterol regulatory element binding protein cleavage-activating protein (SCAP), hydroxymethylglutaryl coenzyme A reductase (HMGCoAR), hydroxymethylglutaryl coenzyme A synthase (HMGCoAS), LDL receptor (LDLR), acetyl-CoA carboxylase (ACC), fatty acid synthase (FAS), glycerol-3-phosphate acyltransferase (GPAT), citrate lyase (CL), malic enzyme (MALIC), phosphoenolpyruvate carboxykinase (PEPCK), and glucose-6-phosphate dehydrogenase (G-6-DH). Results are given as means ± the standard deviation of three independent experiments, each performed in triplicate. Expression levels of indicated enzymes observed in HepG2-pcDNA3 cells were normalized to 1.

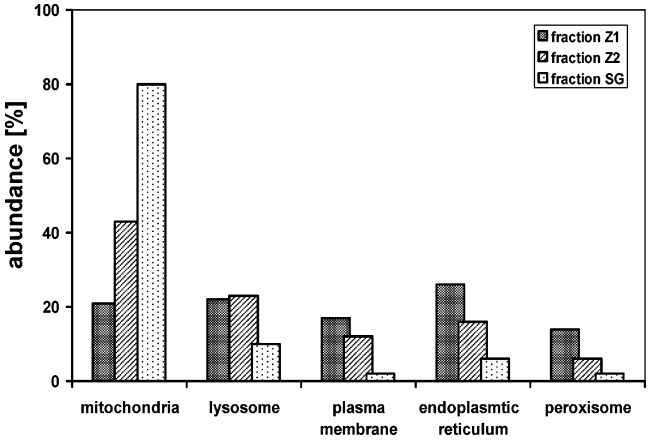

FIGURE 3: Cellular organelle composition in the course of mitochondria preparation. Typical distribution of cellular organelles calculated from marker enzyme data (Table 1) among the fractionation process. Organelle separation was performed by differential centrifugation (Z1, 666*g*; Z2, 11000*g*) and consecutive isopyknic centrifugation (SG) using a linear sucrose gradient (from 0.7 to 1.5 M).

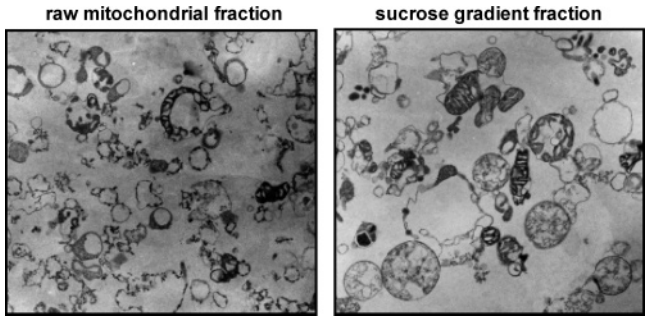

FIGURE 4: Electron micrographs of the main steps in the progress of mitochondrial preparation. Typical micrographs of mitochondrial fractions derived from differential centrifugation (raw mitochondrial fraction; second 11000*g* step) and further purification by isopyknic centrifugation (sucrose gradient fraction). Organelles were fixed in the presence of BSA to achieve clearly separated sample constituents. Magnification of 22000×.

recruited. In this way, we could show that half of the total amount of measured SREBP-1 results from the overexpressed SREBP-1a (data not shown).

Next we examined the functionality of overexpressed SREBP-1a within these cells. For analyzing subcellular localization of expressed SREBP-1a, laser scanning microscopy using a HA tag specific antibody was utilized (Figure 1, top panel). As described for endogenous SREBP-1, our construct not only enters the nucleus but also resides solely in this organelle. Staining of mitochondria pointed out that no significant change in localization or number of this organelle was detectable. To investigate the impact of SREBP-1a on cellular lipid metabolism, SREBP-1a (+) cells were maintained for 9 days under high glucose conditions (20 mM glucose and 20% FCS). Under these culture conditions in contrast to mock transfected cells (HepG2-pcDNA3), in SREBP-1a (+) cells light microscopy visualized massive accumulation of lipid droplets within each cell (Figure 1, bottom panel).

Expression Levels of Metabolic Key Enzymes in SREBP-1a (+) Cells. These microscopic observations implicate a modulation in cellular lipid metabolism. For this purpose, we analyzed the expression levels of the known enzymes regulating the committed steps of carbohydrate and lipid metabolism by real-time PCR (Figure 2). This investigation revealed that in SREBP-1a (+) cells significant elevated levels of RNA expression of acetyl-CoA-carboxylase (ACC), fatty acid synthase (FAS), glycerol-3-phosphate acyltransferase (GPAT), LDL receptor, and phosphoenolpyruvate carboxykinase (PEPCK) were detectable, whereas levels of SREBP-2, sterol regulatory element binding protein cleavage-activating protein (SCAP), HMG-CoA reductase (HMGCoAR), HMG-CoA synthase (HMGCoAS), citrate lyase (CL), malic enzyme (MALIC), and glucose-6-phosphate dehydrogenase (G-6-DH) were unaltered.

Cellular Prefractionation of Cells for Preparing Functional Mitochondria. To elucidate the role of SREBP-1a in regulating proteins involved in β-oxidation, we established a protocol for preparing functional mitochondria. For this, 1×10^7 HepG2-pcDNA3 and SREBP-1a (+) cells were seeded on separate cell culture dishes and maintained for 4 days under standardized conditions in culture media. Subsequently, cells were scraped off and disrupted with a Dounce homogenizer. To remove cell debris, nuclei, and soluble cytosolic proteins, we used differential centrifugation. The cellular homogenate was fractionated, and the resulting crude mitochondrial fraction (11000*g* pellet) was further processed by isopyknic centrifugation using a linear sucrose gradient (from 24 to 54%). To determine the sample composition and to calculate the distribution of cellular organelles in the sample

Table 1: Monitoring of the Subcellular Fractionation Process[a]

A		mitochondria					
		succinate dehydrogenase				JC-1 uptake	
preparation step	total protein (mg)	total activity (μmol/min)	yield (%)	specific activity (μmol mg^{-1} min^{-1})	accumulation factor	specific activity (fluor./mg)	accumulation factor
homogenate	61.0 ± 5.0	871 ± 57	100	15 ± 2.0	1	930 ± 70	1
supernatant at 666*g* (Z1)	32.4 ± 4.8	454 ± 67	52	14 ± 0.6	1	1130 ± 45	1
pellet at 11000*g* (Z2)	14.9 ± 0.5	462 ± 64	53	31 ± 1.9	2	1900 ± 35	2
sucrose gradient (SG)	1.2 ± 0.0	109 ± 29	12.5	93 ± 24	6	3540 ± 610	4

B	lysosomes			plasma membrane			endoplasmic reticulum			peroxysomes		
	acidic phosphatase			alkaline phosphatase			glucose-6-phosphatase			catalase		
preparation step	total activity (μmol/min)	yield (%)	specific activity (μmol mg^{-1} min^{-1})	total activity (μmol/min)	yield (%)	specific activity (μmol mg^{-1} min^{-1})	total activity (nmol/min)	yield (%)	specific activity (nmol mg^{-1} min^{-1})	total activity (milliunits/min)	yield (%)	specific activity (milliunits mg^{-1} min^{-1})
homogenate	75450 ± 1400	100	1250 ± 60	8950 ± 920	100	148 ± 3.5	1815 ± 64	100	30 ± 1.4	188.0 ± 8.0	100	3.1 ± 0.1
supernatant at 666*g* (Z1)	39990 ± 860	53	1250 ± 200	3620 ± 400	40	112 ± 4.0	1150 ± 248	63	34 ± 4.2	63.0 ± 11.0	34	2.0 ± 0.1
pellet at 11000*g* (Z2)	20850 ± 210	28	1400 ± 104	1330 ± 35	15	89 ± 1.4	365 ± 7	20	25 ± 0.7	14.2 ± 1.2	7.3	1.0 ± 0.1
sucrose gradient (SG)	1165 ± 35	1.6	970 ± 28	39 ± 4	0.4	33 ± 3.5	16 ± 2	0.9	13 ± 1.4	0.5 ± 0.1	0.3	0.5 ± 0.1

[a] For preparation of mitochondria, HepG2-pcDNA3 and SREBP-1a (+) cells were maintained for 4 days in culture medium (RPMI 1640 supplemented with 10% FCS). Organelle fractionation by a consecutive centrifugation approach [homogenate; Z1, 666*g*; Z2, 11000*g*; SG, linear sucrose gradient (from 0.7 to 1.5 M)] was carried out under standardized conditions (see Experimental Procedures). Organelle composition in each preparation steps was monitored by dedicated marker enzyme activity assays. For part A, enrichment of intact mitochondria during preparation was monitored by measuring succinate dehydrogenase activity and JC-1 dye uptake. For calculation of the yield and specific mitochondria accumulation, mean values for total protein amount and specific/total activity were derived from three independent experiments. For part B, contaminants (plasma membrane, endoplasmic reticulum, lysosomes, and peroxisomes) were assessed by marker enzyme assays. The yield and specific organelle accumulation were calculated from three independent experiments.

during separation, marker enzyme assays were used (Table 1). When the specific activity of succinate dehydrogenase, the specific marker for mitochondria, was measured, functional mitochondria were detected in a fraction representing 41−42% sucrose. In summary, enrichment of mitochondria in the sucrose gradient fraction was 6-fold with a recovery rate of approximately 13%. To test mitochondrial functionality, JC-1 dye uptake, which works only with an intact membrane potential, was measured. Here we could detect an approximately 4-fold increase during organelle concentration (Table 1A). Finally, the extent of contamination of the resulting mitochondrial fraction by other organelles was calculated from marker enzyme total activities (Table 1B). Figure 3 shows that our protocol resulted in a content of >80% mitochondria. To examine the structural integrity of isolated mitochondria, the preparation was visualized by electron microscopy. Electron micrographs showed the existence of intact double membranes and an internal mitochondrial matrix next to substantial enrichment of mitochondria with minor contaminates by other organelles (Figure 4). Using this approach, functional mitochondria fractions containing more than 80% mitochondria were subjected to comparative protein pattern analysis by 2-DE, enabling us to investigate thousands of proteins in a parallel manner.

Comparative Analysis of the Mitochondrial Protein Pattern by 2D-DIGE. For comparative mitochondrial protein pattern analyses, we utilized two-dimensional difference gel electrophoresis (2D-DIGE). This novel fluorescence-based multiplexing technique for protein labeling in 2D gels offers a wide dynamic range for detection, coseparation of different samples on the same gel, and for the first time the usage of an internal standard for protein quantification with unsurpassed statistical confidence. Accordingly, approximately 0.5 mg protein samples derived from wild-type and SREBP-1a (+) cells were solubilized and labeled with cyanine dyes (Cy3 and Cy5) prior to electrophoretic separation. To account for potential bias in protein labeling through Cy3 and Cy5 specific coupling, portions of each sample were labeled with Cy3 and Cy5 and vice versa. Additionally, equal amounts (25 μg) of both samples were mixed and labeled with Cy2 to generate the internal standard (Table 2).

According to Table 2, equal amounts of the corresponding Cy2−, Cy3−, and Cy5−protein preparations (in sum 150 μg of protein/gel) were mixed and coseparated on four replicate 2D gels covering the pH range of 4−7 (Figure 5). To visualize the protein pattern, each gel was scanned with fluorophore specific excitation and emission wavelengths to acquire three independent images, each specific for the separated Cy-labeled probe. Image analysis, i.e., spot detection, within gels as well as between gels matching with subsequent determination of significant alterations in protein abundances based on normalization by the internal standard was performed automatically by DeCyder due to stringent parameter settings. Accordingly, only those protein spots were selected which were present in all analyzed gel images (12 separate images) and exhibited differences in standardized average spot volume ratios exceeding 1.5. To justify significance, solely spot couples in the replicates were followed up satisfying *t* test values of $<10^{-3}$ (e.g., see Figure 6). Due to these defaults, 117 protein spots of the overall 1371 spots were pointed out to be significantly altered

Table 2: Fluorophore Labeling Scheme and Gel Setup for the 2D DIGE Approach[a]

sample	gel 1	gel 2	gel 3	gel 4
HepG2-pcDNA3	50 μg of protein Cy3	50 μg of protein Cy3	50 μg of protein Cy5	50 μg of protein Cy5
SREBP-1a (+)	50 μg of protein Cy5	50 μg of protein Cy5	50 μg of protein Cy3	50 μg of protein Cy3
internal standard	50 μg of protein Cy2	50 μg of protein Cy2	50 μg of protein Cy2	50 μg of protein Cy2
HepG2-pcDNA3/SREBP-1a (+) (1:1)				

[a] Mitochondrial protein fractions derived from HepG2-pcDNA3 and SREBP-1a (+) cells were labeled with specific fluorophores, Cy3 and Cy5, as indicated. For internal standard preparation, equal amounts of the two samples were mixed and labeled with Cy2. Prior to electrophoretic separation, labeled samples (Cy3 or Cy5) and the internal standard (Cy2), 50 μg each, were combined according to the scheme and proceeded on four different gels.

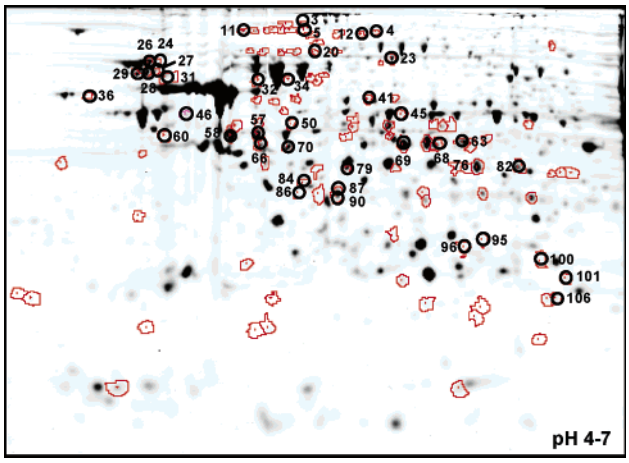

FIGURE 5: Mitochondrial protein profiling by 2D-DIGE. Typical 2-DE protein pattern [cyanine flurophore specific (Cy3, 50 μg protein load) image] of purified mitochondria protein extracts (see Experimental Procedures) derived from HepG2-pcDNA3 and SREBP-1a (+) cells and separated on a 24 cm IPG strip covering the pH range of 4−7 (see Experimental Procedures). Automated image analysis by DeCyder (Amersham Biosciences) detected and matched 1371 protein spots over all 12 single-gel images. Thereby, 117 protein spots show differences in average ratios of a factor at least of 1.5-fold (t test value of $<10^{-3}$ in four parallel gels; 12 separate images) marked by line drawing of spot boundaries. Protein spots circled with a thick line are labeled (see Table 1) and were identified by MALDI-TOF (see Experimental Procedures).

between mitochondrial protein profiles; i.e., 97 spots were more intense in wild-type cells, and 20 spots were more intense in SREBP-1a (+) cells.

Identification of Differentially Expressed Protein Spots by Matrix-Assisted Laser Desorption Ionization (MALDI) Mass Spectrometry. Consecutively, 65 protein spots were excised from coomassie restained DIGE gels and subjected to in-gel digestion with trypsin. Resulting peptides then were applied to peptide mass fingerprint analysis by MALDI-MS. In a search of the NCBI nonredundant database, peptide mass information identified 40 (position marked in Figure 5 by circles and numbers) of the 65 analyzed protein spots, assigning them to 35 distinct proteins (summarized in Table 3). For 25 spots, MS data could not be matched to any known protein, although usable mass spectra were recorded. Glucosidase II, BIP, HSP 70/5, agmatinase, alanyl-tRNA synthase, and pyruvate dehydrogenase were each represented by two separate protein spots. Furthermore, HSP70/1B and T-Plastin were identified in the same protein spot.

Putative Physiological Role of Alterations in the Mitochondrial Protein Pattern in the Cellular Fatty Acid Pattern. According to database entries identified proteins were assigned to their subcellular location and function (Figure 7). Sixty-eight percent of the identified proteins were allocated to mitochondria, whereas only 15% of the proteins were shown to be located in the endoplasmatic reticulum (6%) and cytoskeleton (9%). For 17%, no relation to their localization could be determined (Figure 7A). Grouping mitochondrial proteins according to their specified function revealed that the major part of identified proteins was directly (fatty acid synthesis and β-oxidation) or indirectly (energy budget and Krebs cycle) engaged in lipid metabolism (nearly 40%) or protein synthesis (17%) and protein processing (13%) (Figure 7B).

To examine possible physiological consequences of these changes in the abundance of enzymes related to lipid metabolism (Table 3), we analyzed the cellular lipid content. Measurement of the cholesterol level showed no significant differences between HepG2-pcDNA3 and SREBP-1a (+) cells (data not shown). For analyzing cellular fatty acid content and composition, we have utilized lipid profiling by gas chromatography (Figure 8). First, we have determined the cellular content of total fatty acids (TFA) next to free fatty acids (FFA). This analysis revealed that the absolute TFA level was significantly (>1.5-fold) elevated in cells overexpressing SREBP-1a (Figure 8A). In contrast, the cellular content of FFA was not different between wild-type and SREBP-1a (+) cells. Furthermore, we have analyzed the relative composition of fatty acids within TFA and FFA in percent. Interestingly, the relative percentage composition of fatty acids within TFA was significantly altered in SREBP-1a (+) cells; i.e., levels of palmitic acid (16:0) and stearic acid (18:0) were significantly reduced, whereas levels of oleic acid (18:1), linolic acid (18:3), and arachidonic acid (20:4) were significantly elevated (Figure 8B). In contrast, the relative percentage composition of FFA was unaffected by SREBP-1a.

DISCUSSION

The basic helix−loop−helix transcription factor SREBP-1a is known to regulate a wide range of lipogenic and cholesterogenic enzymes. To dissect the influence of this regulatory protein on complex cellular features in more detail, we generated human liver cells overexpressing the N-terminal domain of SREBP-1a. This model enables investigation of SREBP-1a specific changes in the context of intact human cells due to an overall identical genetic background. Moreover, these cells allow standardized culturing and experimental processing. Accordingly, the system ensures that potentially observed alterations, e.g., in protein profiles, are definitely due to different cellular amounts of SREBP-1a and are not affected by environmental conditions or biological variability.

Laser scanning microscopy shows that the N-terminal HA tag does not affect the import of our SREBP-1a construct

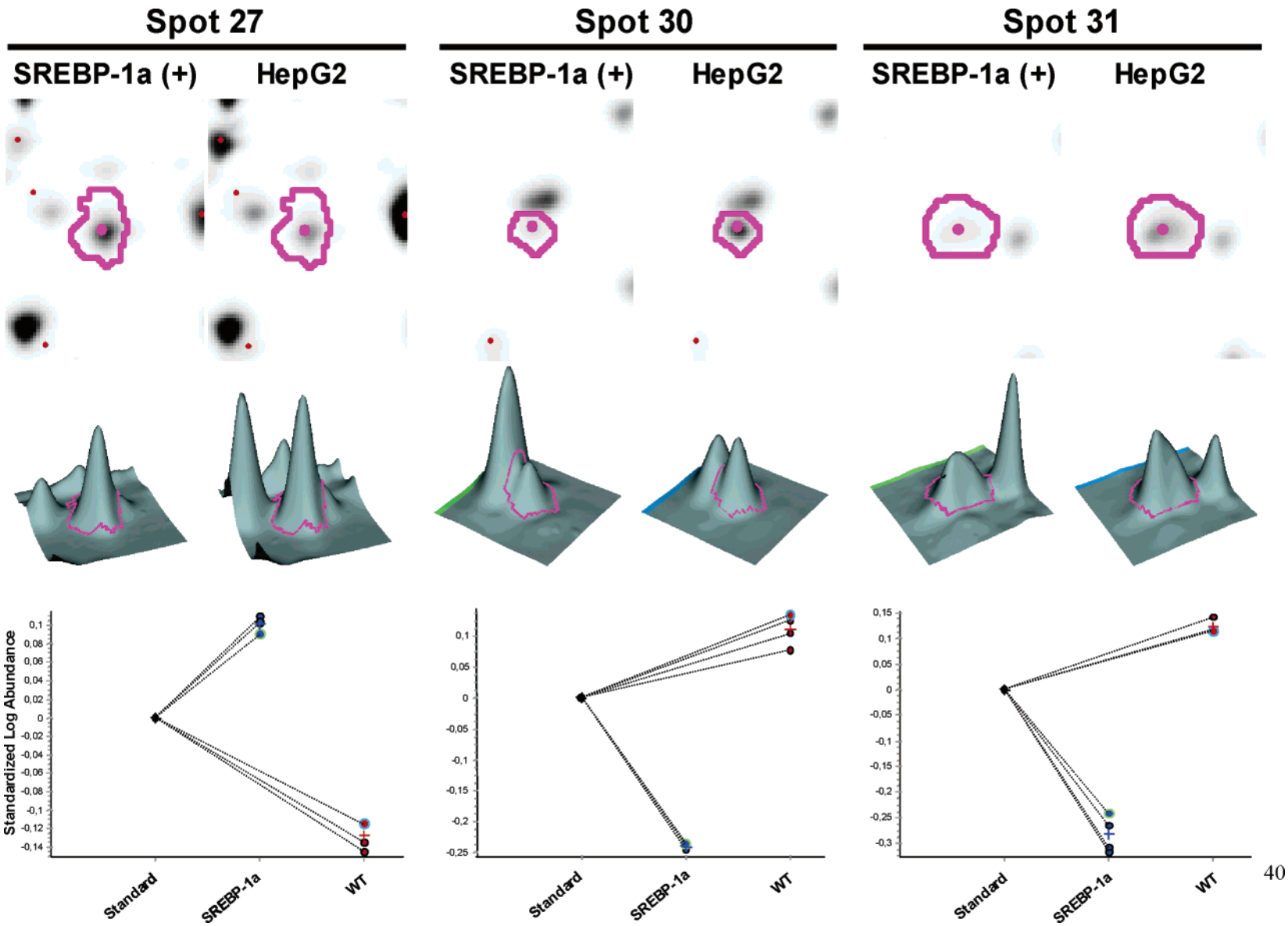

FIGURE 6: Comparison analyses of protein spot intensities by DeCyder. Examples for the evaluation by DeCyder of alterations in spot intensities using the DIGE system are displayed. Spot information of three selected spots, i.e., 27, 30, and 31 (according to Table 3), derived from HepG2 and SREBP-1a (+) cells is shown. The top panel displays partial views of dedicated 2DE images. Spot boundaries of selected protein spots detected by DeCyder are indicated. To point out alterations in corresponding spot intensity proportions, the selected spots are displayed as three-dimensional (3D) images in the middle panel. 3D images were rotated to allow optimal perception. The bottom panel shows associated graph views of standardized log abundances of the selected spots among analyzed gel replicates.

Table 3: List of Proteins Known To Be Different between HepG2 Wild-Type Cells and HepG2 Cells Overexpressing SREBP-1a-NT[a]

protein ID	protein AC	protein name	*p* value	avg SREBP-1a (+)/HepG2 ratio
	Protein Spots whose Intensity in the Mitochondria Protein Pattern Increases (a factor of >1.5) in SREBP-1a (+)			
4	gi|2274968	glucosidase II	9.4e-005	1.57
24	gi|16507237	HSP70 5	2.9e-005	1.62
26	gi|16507237	HSP70 5	6.6e-006	1.54
31	gi|33331032	transglutaminase	0.00014	1.56
57	gi|23831297	AMP phosphotransferase	1.8e-006	1.73
58	gi|4894215	vinexin β	2.2e-007	1.89
68	gi|4505685	pyruvate dehydrogenase	0.00024	1.54
69	gi|4505685	pyruvate dehydrogenase	1.5e-007	1.69
87	gi|18031951	agmatinase	2.1e-009	1.79
90	gi|18031951	agmatinase	0.00012	1.74
	Protein Spots whose Intensity in the Mitochondria Protein Pattern Decreases (a factor of >1.5) in SREBP-1a (+)			
3	gi|38569417	alanyl-tRNA synthetase	6.6e-007	−1.90
5	gi|38569417	alanyl-tRNA synthetase	0.00011	−1.70
11	gi|4557871	transferrin	1.1e-007	−1.64
12	gi|2274968	glucosidase II	0.00036	−2.83
20	gi|8131894	mitofilin	3.2e-005	−1.54
23	gi|543064	long-chain fatty acid β-oxidation complex	1.9e-005	−1.80
27	gi|1346669	NADPH oxidase factor 2	5.1e-008	−2.53
28	gi|20178330	aspartyl-tRNA synthetase	3.0e-007	−2.42
29	gi|6470150	BIP	2.5e-005	−1.69
32	gi|4885431/gi|2506254	HSP70 1B/T-plastin	2.3e-006	−2.29
34	gi|14916998	glutathione reductase	3.8e-007	−2.82
36	gi|6470150	BIP	0.00038	−1.56
41	gi|303618	phospholipase C	9.7e-006	−2.27
45	gi|29840846	mitochondrial processing protease	8.5e-007	−2.01
46	gi|4504161	G-rich RNA binding factor	2.1e-005	−1.55
50	gi|24431966	stress 70 protein chaperone	6.6e-006	−1.52
60	gi|5231269	malonyl-CoA decarboxylase	0.0009	−1.64
63	gi|1168056	ornithine aminotransferase	3.7e-009	−1.98
66	gi|189774	12-lipoxygenase	1.1e-005	−1.57
70	gi|40787805	ribosomal protein S27	6.1e-009	−2.91
76	gi|21396487	hypothetical protein	6.4e-007	−1.87
79	gi|4501859	acyl-coenzyme A dehydrogenase	1.6e-007	−2.25
82	gi|21314961	succinyl-CoA ligase	7.1e-007	−2.53
84	gi|4506667	ribosomal protein PO	2.7e-005	−1.50
86	gi|4826659	F-capping	7.9e-007	−3.09
95	gi|13654294	hypothetical protein	3.0e-005	−2.23
96	gi|14198377	ethylmalonic protein	1.6e-005	−1.78
100	gi|5174743	ubiquinol cytochrome *c* reductase	4.1e-005	−1.81
101	gi|15721937	ribosomal protein S24	5.4e-005	−2.60
106	gi|12005991	mitogaligin	1.7e-005	−2.45

[a] For protein identification, peptides derived from in-gel digestion were analyzed using MALDI-MS. For the protein database search, MASCOT (Matrix Science) was used and adapted to the following criteria: Mascot score higher than 80 and mass tolerance of 150 ppm. Identified proteins are specified by NCBI sequence ID and sorted by protein ID according to the numbering in Figure 1. Classification of protein spots that are different between the two cell lines was based on calculated average ratios by DeCyder (Amersham biosciences) fitting at the following thresholds: protein spots were present in all analyzed gels, standardized average spot volume ratios exceeded 1.5-fold, and *p* values were less than 10^{-3} in four parallel gels.

into the nucleus. In fact, localization of our construct complies like that of endogenous SREBP-1a (*21*). Maintaining these cells in culture medium supplemented with high glucose results in the massive accumulation of lipids within droplets. In contrast in mock transfected cells, this structure is not visible. This observation is consistent with results for this isoform of the SREBP-1 gene examined in different models, e.g., transgenic animals overexpressing SREBP-1a tissue specific in liver or adipocytes which induces elevated rates of fatty acid synthesis and accumulation of lipids (*22*−*24*). In contrast, mice overexpressing the isoform SREBP-1c tissue specific in adipocytes show no accumulation but rather a drastic reduction in intracellular lipid content (*24*), underlining the distinct role of SREBP-1a in lipid metabolism.

Because SREBP-1a is a master regulator of cellular lipid metabolism, accumulation of intracellular lipids due to increased levels of SREBP-1a indicates a disarrangement of fatty acid generation, their intracellular transport, or rate of degradation. This might be caused by changes in activity or abundance of proteins engaged in lipid metabolism. In our investigation, we focus on the abundance of proteins and here on the subproteome of mitochondria, the central organelle in lipid metabolism. Analyzing cellular subproteomes prevents one of the most limiting factors of 2-DE, i.e., poor resolution and dynamic range of detection, failing to visualize the broad range of cellular proteins (structural proteins with 10 000 copies per cell next to regulatory proteins with several copies per cell) simultaneously. Accordingly, analyzing fractionated cellular organelles reduces sample complexity in association with the opportunity to analyze low-abundance proteins.

This strategy enables a detailed analysis of protein structure−function relationships in a physiological context combined with increased power of resolution by fractionating cellular organelles. For this purpose, we established an

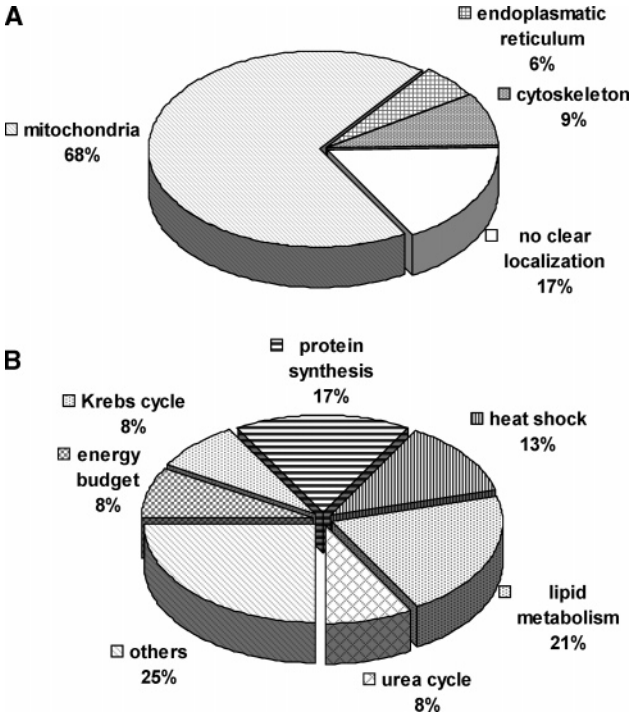

FIGURE 7: Classification of identified proteins. The total amount of 35 distinct proteins was set to 100%. (A) Subcellular localization of identified proteins according to database entries. (B) Putative function of mitochondrial proteins (selected from panel A) according to database entries.

organelle preparation protocol for acquiring reproducible basis material for protein profiling. For control of workmanship, all preparation steps were monitored closely by a broad set of marker enzyme assays, organelle vitality tests, and electron microscopy to control structural integrity, revealing a highly enriched and functional mitochondrial fraction.

Today for proteome wide quantitative protein profiling, several complementary approaches are available, e.g., 2-DE, LC−MS/MS, SELDI, and protein arrays. Until now, the 2-DE technique offered the greatest power of separation for a comparative analysis of complex protein samples. But gel-based proteome analysis is restricted by its complexity of sample processing, whereby reproducibility is noted as the crucial item for any reliable comparable proteome analysis. Protein profiling by standard gel-based 2-DE approaches requires comparison of protein patterns separated on physically different gels (one sample per gel), which exhibits several system-dependent difficulties, i.e., substantial gel-to-gel variations due to protein loading and staining inconsistencies. Moreover, local as well as global distortions of the gel matrix constrict precise matching of spot patterns among different gels. In accordance with that, accurate computer-aided image analyses for detecting alterations in protein spot quantities with adequate statistical confidence are impaired. Especially in the case of weak spots located near the detection limit, spot intensities of corresponding spots among different gels vary by a factor of up to 10 even if the identical sample is processed under standardized conditions (*25*). Also, recruiting large sets of gels to work with statistical filtered spot data fails to determine small differences between protein spot intensities, which are situated in the range of a factor of 2.5. Considering the fact that the crucial factor for gel-based comparative proteome

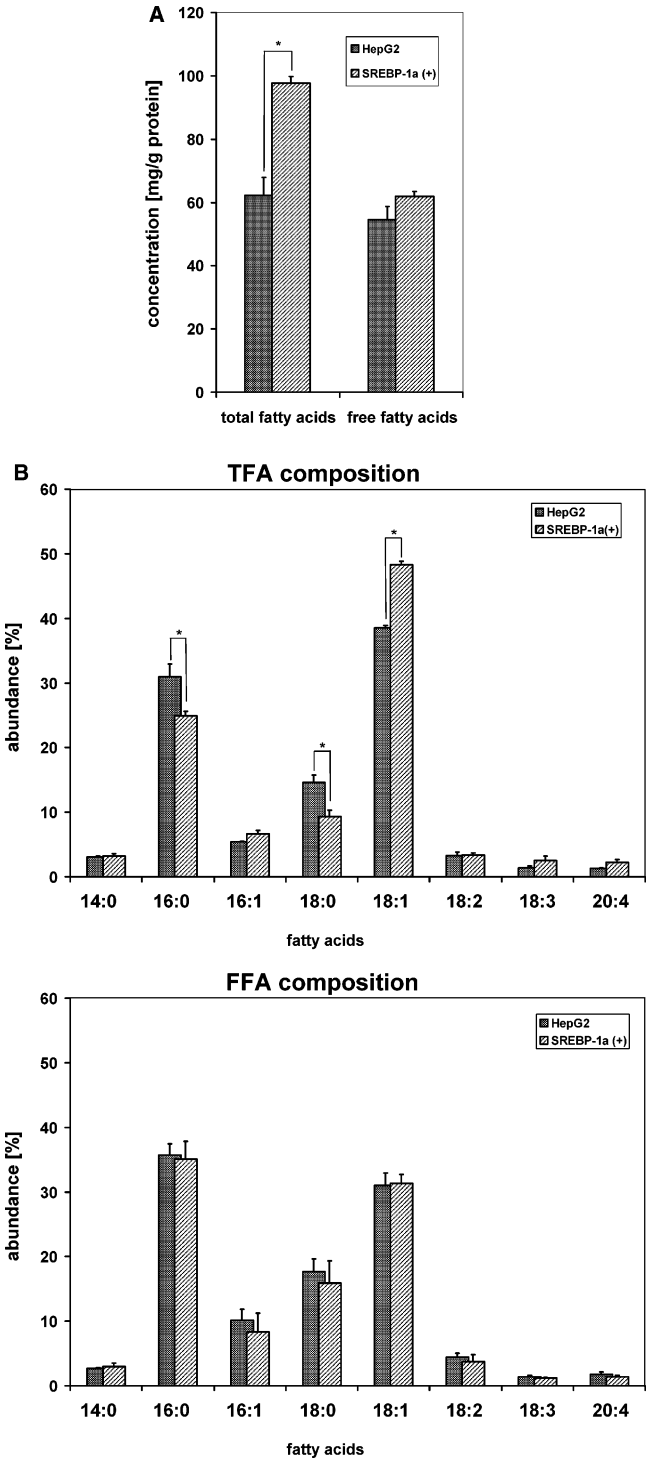

FIGURE 8: Cellular lipid content and composition of SREBP-1a (+) cells. For determination of cellular total fatty acid (TFA) and free fatty acid (FFA) content and composition, cells were maintained in culture medium (RPMI 1640 with 10% FCS) for 4 days. HepG2-pcDNA3 and SREBP-1a (+) cells (1×10^7) subsequently were subjected to analysis by gas chromatography (see Experimental Procedures). Mean values for the percentage distribution of six independent experiments are displayed. (A) Absolute content (milligrams of fatty acid per gram of total protein) of TFA and FFA in HepG2 and SREBP-1a (+) cells. (B) Percentage fatty acid composition of TFA and FFA in HepG2 and SREBP-1a (+) cells. The sum of measured fatty acids was set to 100%. Asterisks indicate significant changes in fatty acid content ($p < 0.01$).

analysis is reproducibility, we applied Ettan-DIGE technology, a novel fluorescence-based multiplexing technique for

protein labeling in 2D gels for protein separation, detection, and determination of differences in protein profiles. Next to high sensitivity (requiring only 50 μg of protein per sample and gel) and a wide linear dynamic range of detection (4 orders of magnitude), this technique provides coseparation of different samples on the same gel (multiplexing), preventing gel-to-gel variations per se. Because variation of spot intensities due to gel specific experimental factors will be identical for all samples run on a particular gel, the relative amounts of a specific protein in the samples will be unaffected. As an outstanding feature, this system utilizes for the first time an in-gel standard assembled out of equal portions of analyzed samples (*26*). This internal standard is coseparated on each gel and used for normalization and calculation of protein abundance among different replicate gels. Utilization of this feature provides unsurpassed statistical confidence for determination of alterations in protein abundances, which allow identification of differences as small as a factor of 1.2.

Using this DIGE approach, comparative protein analysis of mitochondrial protein profiles derived from mock transfected HepG2 and SREBP-1a cells detected approximately 1400 different protein spots spanning the pH range of 4−7. Quantification by DeCyder image analysis software revealed that 117 distinct protein spots were pointed out to be significantly altered (factor of 1.5) between the two protein patterns. Interestingly, the predominant part of altered protein spots exhibited only a small difference in normalized average spot ratios near a factor of 1.5-fold. None of them exceeded a factor of 3. Therefore, determination of those alterations was solely enabled by utilizing the DIGE approach, whereas in this case, a classic "one sample per gel" approach would fail to give a serious statement. Here the substantial gel-to-gel variations inherently exceeded the default thresholds. Therefore, the DIGE technique opens a new dimension for monitoring regulation processes within the cell.

Several proteins (glucosidase II, BIP, HSP 70/5, agmatinase, alanyl-tRNA synthase, and pyruvate dehydrogenase) are represented by more than one distinct protein spot. This phenomenon might be based on a shift in molecular weight or isoelectric point due to posttranslational modification (e.g., phosphorylation or glycosylation). As a principle of 2D-PAGE, those changes in molecular mass or isoelectric point are detectable. In the case of glucosidase II, the examination of expression data revealed that in SREBP-1a (+) cells the protein is simultaneously increased in one protein spot and decreased in another protein spot. This may indicate a genotype specific appearance of different modified glucosidase II isoforms.

On the basis of alterations between HepG2 and SREBP-1a (+) cells determined by image analysis by DeCyder and peptide mass fingerprint analysis, only 15% of the identified proteins (Table 3) were assigned to a nonmitochondrial context (endoplasmatic reticulum or cytoskeleton), reflecting the high quality of sample preparation. Among the mitochondrial proteins affected by an elevated level of expression of SREBP-1a, 21% of identified mitochondrial proteins are enzymes engaged in lipid metabolism.

Interestingly, in SREBP-1a (+) cells several protein spots representing enzymes in key positions of lipid metabolism are significantly altered, i.e., pyruvate dehydrogenase and succinyl-CoA ligase or malonyl-CoA decarboxylase. The enzyme pyruvate dehydrogenase is more abundant in SREBP-1a (+) cells and provides source material for the Krebs cycle, whereas succinyl-CoA ligase forces the Krebs cycle but is less abundant. Therefore, citrate levels in the mitochondria possibly increase. To overcome this enrichment, citrate will be transported to the cytosol and will be metabolized to acetyl-CoA, the source of fatty acid synthesis. Beyond this, malonyl-CoA decarboxylase, an enzyme that affects lipid partitioning (*27*) and seems to be less abundant in the SREBP-1a (+) cells, also triggers cellular lipid metabolism instead of accumulation of fatty acids or its degradation. These observations agree with results from gene expression data provided by us and others (*28*−*31*). RNA expression levels of cytosolic enzymes regulating the committed steps for synthesis of lipids exhibit a significant increase with overexpression of SREBP-1a. Moreover, our mitochondrial subproteome analyses additionally show that several protein spots representing enzymes in key positions of β-oxidation are significantly less abundant in SREBP-1a (+) cells. These different acyl-CoA dehydrogenases, catalyzing first steps in β-oxidation, indicate a decreased level of degradation of fatty acids in mitochondria.

Summarizing our results suggests a more complex regulation of lipid homeostasis, i.e., participation of key enzymes associated with β-oxidation and lipid portioning. As biological readout, we performed GC analyses of lipid content and composition. This investigation pointed out that only TFA content is significantly elevated by overexpressing SREBP-1a, whereas FFA content was unaffected. In addition to a significant increase in TFA content, its fatty acid composition is shifted to an accumulation of unsaturated long-chain fatty acids (18:1, 18:3, and 20:4). In contrast, the fatty acid pattern of FFA shows no alteration. This elevated TFA content is consistent with the observation made by light microscopy. Here we have detected massive accumulation of lipid droplets within the SREBP-1a cells. In combination with our protein profiling data, observed elevated levels of TFA associated with alterations in their composition indicate a direct involvement of mitochondrial lipid metabolism in the context of SREBP-1a action.

ACKNOWLEDGMENT

We thank L. Kuehn (German Diabetes Center) for kind preparation of mitochondria samples and F. Kopp (German Diabetes Center) for performing electron microscopy.

REFERENCES

1. Briggs, M. R., Yokoyama, C., Wang, X., Brown, M. S., and Goldstein, J. L. (1993) Nuclear protein that binds sterol regulatory element of low-density lipoprotein receptor promoter. I. Identification of the protein and delineation of its target nucleotide sequence, *J. Biol. Chem. 268*, 14490−14496.
2. Wang, X., Briggs, M. R., Hua, X., Yokoyama, C., Goldstein, J. L., and Brown, M. S. (1993) Nuclear protein that binds sterol regulatory element of low-density lipoprotein receptor promoter. II. Purification and characterization, *J. Biol. Chem. 268*, 14497−14504.
3. Hua, X., Yokoyama, C., Wu, J., Briggs, M. R., Brown, M. S., Goldstein, J. L., and Wang, X. (1993) SREBP-2, a second basic-helix-loop-helix-leucine zipper protein that stimulates transcription by binding to a sterol regulatory element, *Proc. Natl. Acad. Sci. U.S.A. 90*, 11603−11607.

4. Tontonoz, P., Kim, J. B., Graves, R. A., and Spiegelman, B. M. (1993) ADD1: A novel helix-loop-helix transcription factor associated with adipocyte determination and differentiation, *Mol. Cell. Biol. 13*, 4753−4759.
5. Yokoyama, C., Wang, X., Briggs, M. R., Admon, A., Wu, J., Hua, X., Goldstein, J. L., and Brown, M. S. (1993) SREBP-1, a basic-helix-loop-helix-leucine zipper protein that controls transcription of the low-density lipoprotein receptor gene, *Cell 75*, 187−197.
6. Brown, M. S., and Goldstein, J. L. (1999) A proteolytic pathway that controls the cholesterol content of membranes, cells, and blood, *Proc. Natl. Acad. Sci. U.S.A. 96*, 11041−11048.
7. Kotzka, J., Lehr, S., Roth, G., Avci, H., Knebel, B., and Muller-Wieland, D. (2004) Insulin-activated Erk-mitogen-activated protein kinases phosphorylate sterol regulatory element-binding protein-2 at serine residues 432 and 455 in vivo, *J. Biol. Chem. 279*, 22404−22411.
8. Roth, G., Kotzka, J., Kremer, L., Lehr, S., Lohaus, C., Meyer, H. E., Krone, W., and Muller-Wieland, D. (2000) MAP kinases Erk1/2 phosphorylate sterol regulatory element-binding protein (SREBP)-1a at serine 117 in vitro, *J. Biol. Chem. 275*, 33302−33307.
9. Kotzka, J., Muller-Wieland, D., Roth, G., Kremer, L., Munck, M., Schurmann, S., Knebel, B., and Krone, W. (2000) Sterol regulatory element binding proteins (SREBP)-1a and SREBP-2 are linked to the MAP-kinase cascade, *J. Lipid Res. 41*, 99−108.
10. Kotzka, J., Muller-Wieland, D., Koponen, A., Njamen, D., Kremer, L., Roth, G., Munck, M., Knebel, B., and Krone, W. (1998) ADD1/SREBP-1c mediates insulin-induced gene expression linked to the MAP kinase pathway, *Biochem. Biophys. Res. Commun. 249*, 375−379.
11. Schmitz, G., and Torzewski, M. (2002) *HMG-CoA Reductase Inhibitors*, Birkhäuser Verlag, Basel, Switzerland.
12. Amemiya-Kudo, M., Shimano, H., Hasty, A. H., Yahagi, N., Yoshikawa, T., Matsuzaka, T., Okazaki, H., Tamura, Y., Iizuka, Y., Ohashi, K., Osuga, J., Harada, K., Gotoda, T., Sato, R., Kimura, S., Ishibashi, S., and Yamada, N. (2002) Transcriptional activities of nuclear SREBP-1a, -1c, and -2 to different target promoters of lipogenic and cholesterogenic genes, *J. Lipid Res. 43*, 1220−1235.
13. Righetti, P. G., Campostrini, N., Pascali, J., Hamdan, M., and Astner, H. (2004) Quantitative proteomics: A review of different methodologies, *Eur. J. Mass Spectrom. 10*, 335−348.
14. Weston, A. D., and Hood, L. (2004) Systems biology, proteomics, and the future of health care: Toward predictive, preventative, and personalized medicine, *J. Proteome Res. 3*, 179−196.
15. Unlu, M., Morgan, M. E., and Minden, J. S. (1997) Difference gel electrophoresis: A single gel method for detecting changes in protein extracts, *Electrophoresis 18*, 2071−2077.
16. Asirvatham, V. S., Watson, B. S., and Sumner, L. W. (2002) Analytical and biological variances associated with proteomic studies of *Medicago truncatula* by two-dimensional polyacrylamide gel electrophoresis, *Proteomics 2*, 960−968.
17. Gade, D., Thiermann, J., Markowsky, D., and Rabus, R. (2003) Evaluation of two-dimensional difference gel electrophoresis for protein profiling. Soluble proteins of the marine bacterium *Pirellula* sp. strain 1, *J. Mol. Microbiol. Biotechnol. 5*, 240−251.
18. Pennington, R. J. (1961) Biochemistry of dystrophic muscle. Mitochondrial succinate-tetrazolium reductase and adenosine triphosphatase, *Biochem. J. 80*, 649−654.
19. Bergmeyer, H. U. (1974) *Methoden der Enzymatischen Analyse*, Verlag Chemie, Weinheim, Germany.
20. Aebi, H. (1984) Catalase in vitro, *Methods Enzymol. 105*, 121−126.
21. Sato, R., Yang, J., Wang, X., Evans, M. J., Ho, Y. K., Goldstein, J. L., and Brown, M. S. (1994) Assignment of the membrane attachment, DNA binding, and transcriptional activation domains of sterol regulatory element-binding protein-1 (SREBP-1), *J. Biol. Chem. 269*, 17267−17273.
22. Shimano, H., Horton, J. D., Hammer, R. E., Shimomura, I., Brown, M. S., and Goldstein, J. L. (1996) Overproduction of cholesterol and fatty acids causes massive liver enlargement in transgenic mice expressing truncated SREBP-1a, *J. Clin. Invest. 98*, 1575−1584.
23. Shimomura, I., Shimano, H., Korn, B. S., Bashmakov, Y., and Horton, J. D. (1998) Nuclear sterol regulatory element-binding proteins activate genes responsible for the entire program of unsaturated fatty acid biosynthesis in transgenic mouse liver, *J. Biol. Chem. 273*, 35299−35306.
24. Horton, J. D., Shimomura, I., Ikemoto, S., Bashmakov, Y., and Hammer, R. E. (2003) Over-expression of sterol regulatory element-binding protein-1a in mouse adipose tissue produces adipocyte hypertrophy, increased fatty acid secretion, and fatty liver, *J. Biol. Chem. 278*, 36652−36660.
25. Lehr, S., Kotzka, J., Knebel, B., Schiller, M., Krone, W., and Muller-Wieland, D. (2002) Primary skin fibroblasts as human model system for proteome analysis, *Proteomics 2*, 280−287.
26. Alban, A., David, S. O., Bjorkesten, L., Andersson, C., Sloge, E., Lewis, S., and Currie, I. (2003) A novel experimental design for comparative two-dimensional gel analysis: Two-dimensional difference gel electrophoresis incorporating a pooled internal standard, *Proteomics 3*, 36−44.
27. An, J., Muoio, D. M., Shiota, M., Fujimoto, Y., Cline, G. W., Shulman, G. I., Koves, T. R., Stevens, R., Millington, D., and Newgard, C. B. (2004) Hepatic expression of malonyl-CoA decarboxylase reverses muscle, liver and whole-animal insulin resistance, *Nat. Med. 10*, 268−274.
28. Horton, J. D., Shah, N. A., Warrington, J. A., Anderson, N. N., Park, S. W., Brown, M. S., and Goldstein, J. L. (2003) Combined analysis of oligonucleotide microarray data from transgenic and knockout mice identifies direct SREBP target genes, *Proc. Natl. Acad. Sci. U.S.A. 100*, 12027−12034.
29. Horton, J. D., Goldstein, J. L., and Brown, M. S. (2002) SREBPs: Activators of the complete program of cholesterol and fatty acid synthesis in the liver, *J. Clin. Invest. 109*, 1125−1131.
30. Kotzka, J., and Muller-Wieland, D. (2004) Sterol regulatory element-binding protein (SREBP)-1: Gene regulatory target for insulin resistance? *Expert Opin. Ther. Targets 8*, 141−149.
31. Kotzka, J., and Muller-Wieland, D. (2003) Transcription factors as molecular targets for the metabolic syndrome, *Diabetes Stoffwechsel 12*, 291−299.

BI0479656